communications earth & environment

Article

https://doi.org/10.1038/s43247-024-01748-2

The magmatic plumbing beneath the Wudalianchi volcanic region, northeast China, is recharged by magma reservoirs under Keluo volcano

Ziqiang Lü[1], Jianshe Lei[2] ✉, Dapeng Zhao[3], Yi-Gang Xu[4], Lijun Liu[5], Changqing Sun[2], Yinshuang Ai[5] & Tuncay Taymaz[6]

The intraplate magmatic systems of the Wudalianchi potassic volcanic region in northeast China have historically exhibited eruption activity, and there is evidence that they retain the potential for future eruptions. However, the characteristics of this complex volcanic region remain debated and poorly understood due to the relatively low resolution of existing crustal tomography. Here we present a high-resolution shear-wave velocity model of the crust and uppermost mantle obtained by applying full-waveform ambient noise tomography to data recorded at 106 recently deployed broadband seismic stations. Our results reveal two vertical low-velocity anomalies discovered beneath the Nuominhe and Keluo volcanoes, which appear to be magma ascending pathways connecting a mantle source and crustal reservoirs. A horizontally interconnected low-velocity zone in the middle-lower crust indicates a magmatic migration pathway transporting potassium-rich melts directly among the potassic volcanic units. In addition, the Wudalianchi volcano is likely recharged by deeper and larger crustal magma reservoirs under the Keluo volcano. The unique geometries of the magmatic plumbing systems provide valuable seismic evidence for the volcanic eruption dynamics and potential volcanic hazards.

There are many intraplate volcanoes in northeast China, which are located ~1800 km away from the Japan Trench and have erupted episodically from the late Cretaceous to the present[1] (Fig. 1a). These intraplate volcanoes are covered by alkali basalts, which can be divided into sodic volcanic units ($K_2O/Na_2O < 1$) and potassic volcanic units ($K_2O/Na_2O > 1$) in terms of their elemental composition variations[2,3]. The potassic volcanic units (Fig. 1b), including Wudalianchi (WDLC), Erkeshan (EKS), Keluo (KL), Nuominhe (NMH), and Xiaogulihe (XGH)[4], are mainly distributed in the northern margin of the Songliao Basin, as compared with the widespread sodic volcanism (such as the Changbaishan and Jingpohu volcanoes) along the eastern flank of the basin[5,6]. The WDLC volcano is a typical example of the potassic volcanic units, which experienced three exceptional episodes of eruptions from the early Pleistocene to Holocene[7,8]. Its latest eruption occurred in ~1721 and the effusive lava spread over an area of ~68 square kilometers. In 1776, the most recent volcanic activity took place in Laoheishan, a sub-volcano within the WDLC volcanic area[9]. Considering its historic eruption and potential for re-eruption, the WDLC volcanic region is an ideal area for exploring the trans-crustal magmatic systems and monitoring the volcanic activity in northeast China.

A complex volcanic framework typically consists of a deep mantle source and shallow trans-crustal magmatic systems. Although the deep origin and geodynamics of the intraplate volcanoes in northeast China are still controversial[10–13], most of the tomographic results obtained so far indicate that the origin of the WDLC volcanism is related to the northwestward deep subduction of the Pacific plate. However, it is still unclear whether the volcanic units are influenced by a minor or moderate plume,

[1]College of Mining, Liaoning Technical University, Fuxin, China. [2]Key Laboratory of Crustal Dynamics, National Institute of Natural Hazards, Ministry of Emergency Management of China, Beijing, China. [3]Department of Geophysics, Graduate School of Science, Tohoku University, Sendai, Japan. [4]State Key Laboratory of Isotope Geochemistry, Guangzhou Institute of Geochemistry, Chinese Academy of Sciences, Guangzhou, China. [5]Key Laboratory of Earth and Planetary Physics, Institute of Geology and Geophysics, Chinese Academy of Sciences, Beijing, China. [6]Department of Geophysical Engineering, The Faculty of Mines, Istanbul Technical University, Maslak, Sarıyer, 34469 İstanbul, Türkiye. ✉e-mail: jshlei_cj@126.com

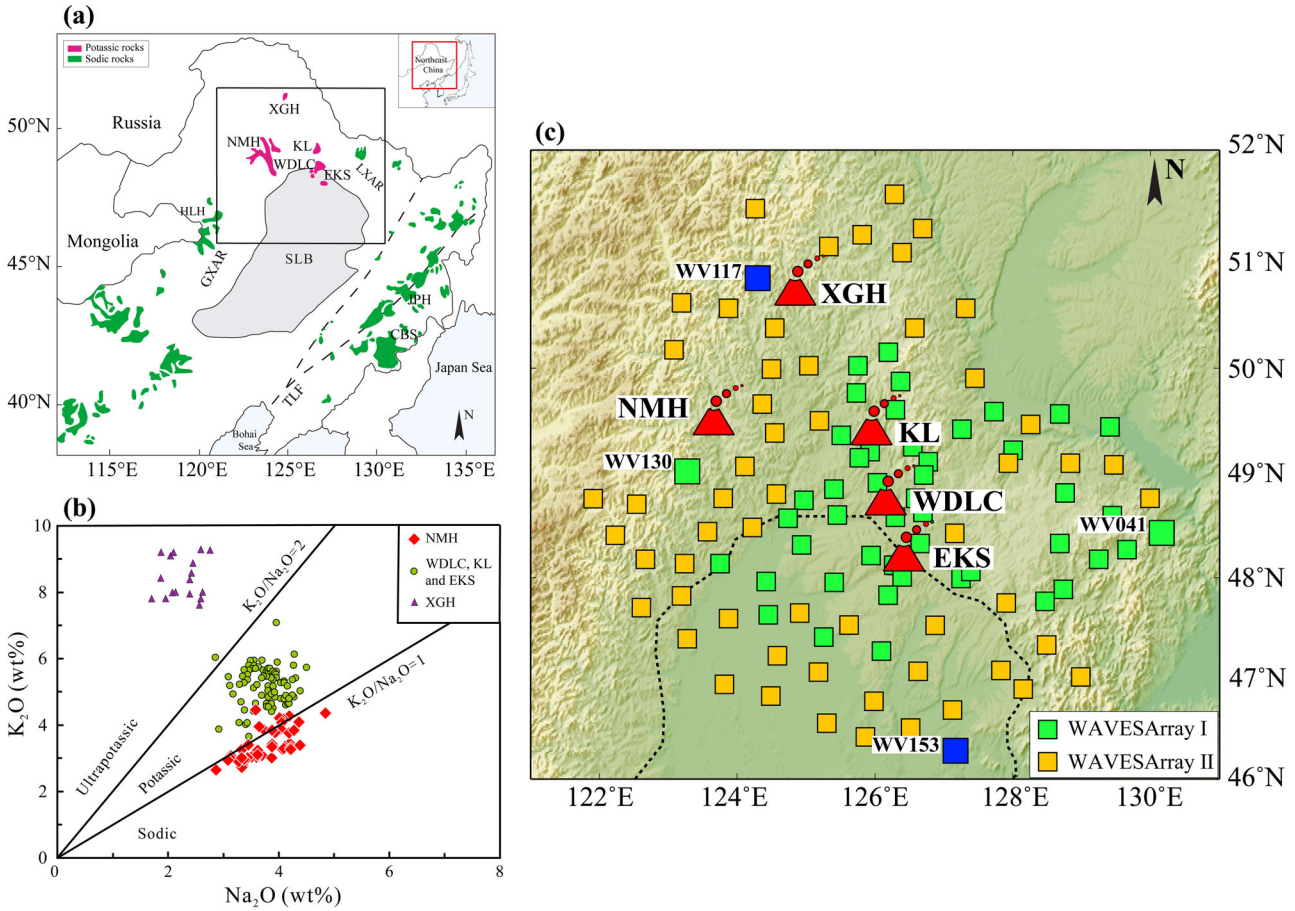

Fig. 1 | Tectonic setting of northeast China and the distribution of seismic stations. a Distribution of the potassic (purple patches) and sodic (green patches) rocks in northeast China. The inset shows the geographic location of the study region. Changbaishan (CBS), Jingpohu (JPH), Halaha (HLH), Great Xing'an Ranges (GXAR), Lesser Xing'an Ranges (LXAR), Songliao basin (SLB), Tanlu fault (TLF). **b** Variations of K_2O versus Na_2O at the Nuominhe (NMH), Xiaogulihe (XGH), Keluo (KL), Wudalianchi (WDLC), and Erkeshan (EKS) volcanoes[4]. **c** Seismic stations used in this study for full-wave ambient noise tomography. The yellow and green squares denote the WAVESArray I and WAVESArray II seismic stations, respectively. The WAVESArray I contains 46 portable stations from August 2015 to April 2019, whereas the WAVESArray II contains 60 temporary stations from July 2016 to April 2019. The blue and green squares mark the locations of the station pairs for waveform fitting in Fig. 2. The red volcanic symbols denote potassic basalt volcanoes.

because the existing tomography models have relatively low resolution in the upper mantle[10,14–16]. From a hazard forecast perspective, many volcanic eruptions are directly influenced by the trans-crustal magmatic system[17]. This system controls the distribution of melts and the physical conditions from slow melt accumulation to rapid melt transfer, as well as the geometry of the magma storage and migration system. Therefore, it is necessary to determine a high-resolution, three-dimensional (3-D) seismic velocity model for better understanding the volcanism of the entire potassic volcanic units in northeast China. However, there is still no such a high-resolution model of the crust and upper mantle beneath the WDLC volcanic area due to the sparse distribution of seismic stations.

The spatial pattern of the vertical trans-crustal pathways and the horizontal plumbing systems of the crustal magma beneath these potassic volcanoes is still unclear. Recent high-resolution ambient noise tomography detected a magma chamber with inferred fluids and partial melts in the shallow crust (~7–13 km depths) beneath the WDLC volcano[18]. Magnetotelluric (MT) inversion also revealed an anomaly modeled as a magma reservoir in the middle crust (~10–15 km depths) recharging the shallow magma chamber[19,20]. However, whether there is a deeper magma reservoir, especially around the crust-mantle boundary, remains ambiguous because the presently available small-scale dense seismic array is only sensitive to the upper-middle crustal structure. Regional-scale ray-based ambient noise tomography revealed a local and relatively weak low-velocity (low-V) anomaly in the lithospheric mantle beneath the WDLC volcano[21]. In contrast, a joint inversion of ambient noise and teleseismic surface waves revealed pervasive low-V anomalies extending down to 200 km depth beneath the WDLC volcano and its adjacent areas[22]. However, the ray-based seismic tomography has difficulties in resolving small-scale low-V anomaly patterns and amplitudes due to the wavefront healing effect[23,24]. Moreover, all the previous seismic models have limited resolution for the entire potassic volcanic region, and cannot resolve more details of structural anomalies, which hamper further understanding of the trans-crustal magmatic systems of the potassic volcanoes in northeast China.

With the enhancement in the WAVESArray seismic station coverage, 106 temporary broadband seismometers were deployed by the National Institute of Natural Hazards, Ministry of Emergency Management of China from August 2015 to April 2019, covering the entire potassic volcanic region (Fig. 1c). This provides an opportunity to elucidate the detailed trans-crustal structure of the potassic volcanoes in northeast China. Here we present new high-resolution seismic images of the crust and uppermost mantle obtained with the full-waveform ambient noise tomographic method[25–29]. This method adopts a special frequency-time-normalization technique to retrieve high-quality Rayleigh wave empirical Green's functions (EGFs) at 5–40 s periods[30] (Supplementary Fig. 1), calculates 3-D finite-frequency sensitivity of

Rayleigh wave rather than seismic rays[31], inverts the sensitivity of Rayleigh wave for both P and S wave velocity (Vp, Vs) perturbations with a set of smoothing and damping parameters, and therefore improves the model accuracy (Supplementary Figs. 2–4). The 3-D Vs model is then updated progressively by reducing the misfit between the observed EGFs and synthetic waveforms. Our new tomographic result evidently delineates the deep interactive characteristics of the entire potassic volcanic units and presents important clues for monitoring the potential eruption risk of the WDLC volcano in the future. Our high-resolution tomography of the crust and uppermost mantle provides new insight into the trans-crustal magmatic system beneath the potassic volcanoes in northeast China.

Results and discussion

Seismic images of the WDLC potassic volcanic region

By integrating our latest dense WAVESArray broadband seismic array, we can now accurately distinguish finer-scale seismic features with a horizontal resolution of ~40 km (Supplementary Figs. 5 and 6). We compare our model with the initial reference model[32–35], demonstrating that the final tomographic model does not rely on seismic features in the initial reference model (Supplementary Figs. 7–11). Our tomographic results reveal several trans-crustal features beneath the WDLC volcano and its adjacent areas (Fig. 2). The shallow crustal velocity structures are well correlated with the regional surface topography. Low-V anomalies are imaged beneath the Songliao Basin, laterally coincident with the outline of the basin, and high-velocity (high-V) anomalies are imaged beneath the major mountain belts. In the middle crust, relatively low-V anomalies exist below the WDLC-NMH-XGH volcanic areas with uneven patterns, and those low-V anomalies appear to horizontally interconnect between the volcanoes. Specially, a low-V zone at depths of ~15–30 km appears to be relatively strong and horizontally connected between the potassic volcanoes (Fig. 3). Near the crust-mantle boundary, prominent high-V anomalies exist (Fig. 2c), which could be associated with ancient remnant structures, resulting from cooling of the lithosphere since rifting ceased about 100 Ma[36]. Two channel-shaped relatively weak low-V anomalies ascend from the uppermost mantle beneath the NMH and KL volcanoes (Fig. 3a), which may reflect vertical pathways for magma upwelling. Very strong high-V anomalies extend from the Songliao Basin to the WDLC volcano in a depth range of ~30–45 km (Fig. 3c, d). Similar high-V anomalies in the uppermost mantle beneath the WDLC volcanic region were also revealed by previous studies using different datasets and tomographic methods[37,38]. The newly detected structural variations suggest that the magmatic systems beneath the potassic volcanoes in northeast China have unique features.

A series of uncertainty estimates and recovery tests are performed to evaluate the reliability and spatial resolution of our tomographic model. The misfit between the synthetics for the inverted 3-D Vs model and the observed EGFs decreases after four iterations. In comparison with those for the initial reference model[32], the final phase delays are gradually minimized and less scattered at all period bands (Supplementary Figs. 2 and 3). The synthetic waveforms for the final Vs model match the observed EGFs well (Fig. 2e, f), indicating that the improved Vs model is more reliable and compatible with the EGFs observations. To further validate the reliability of the key structural features, we perform specific model recovery tests in terms of amplitude and geometry between the potassic volcanoes, including the horizontally connected low-V anomalies in the middle to lower crust and vertical magmatic pathways near the

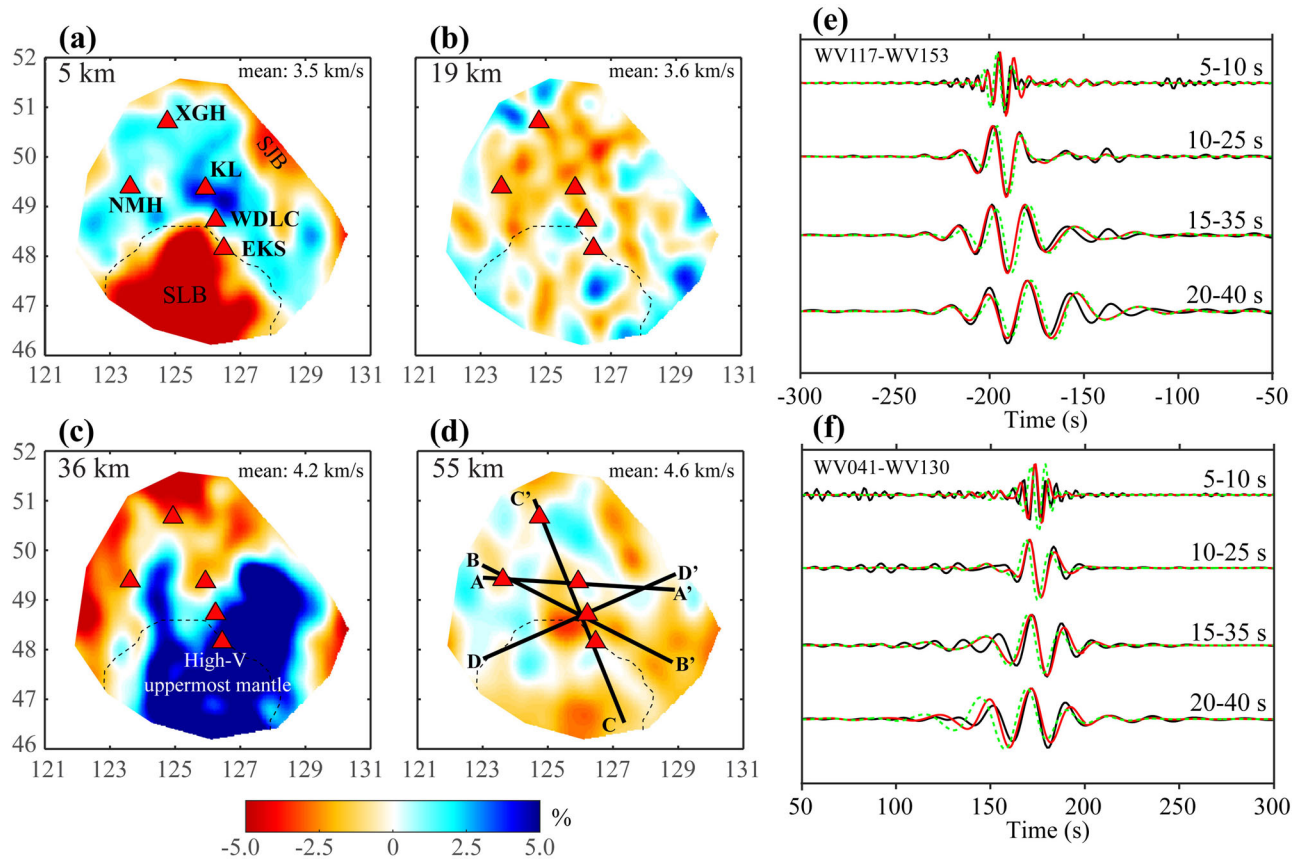

Fig. 2 | Shear-wave velocity model and waveform fitting. a–d Velocity slices shown at depths of 5 km, 19 km, 36 km, and 55 km, respectively. The red triangles represent the potassic basalt volcanoes. The thick black lines in (**d**) mark the profile locations in Fig. 3. **e**, **f** Waveform fitting between observed EGFs and synthetic waveforms at different period bands. The black lines denote the observed EGFs. The red solid lines and the green dashed lines represent synthetic waveforms for the final model and the initial model, respectively. Locations of the station pairs are shown in Fig. 1c. Other symbols are the same as in Fig. 1.

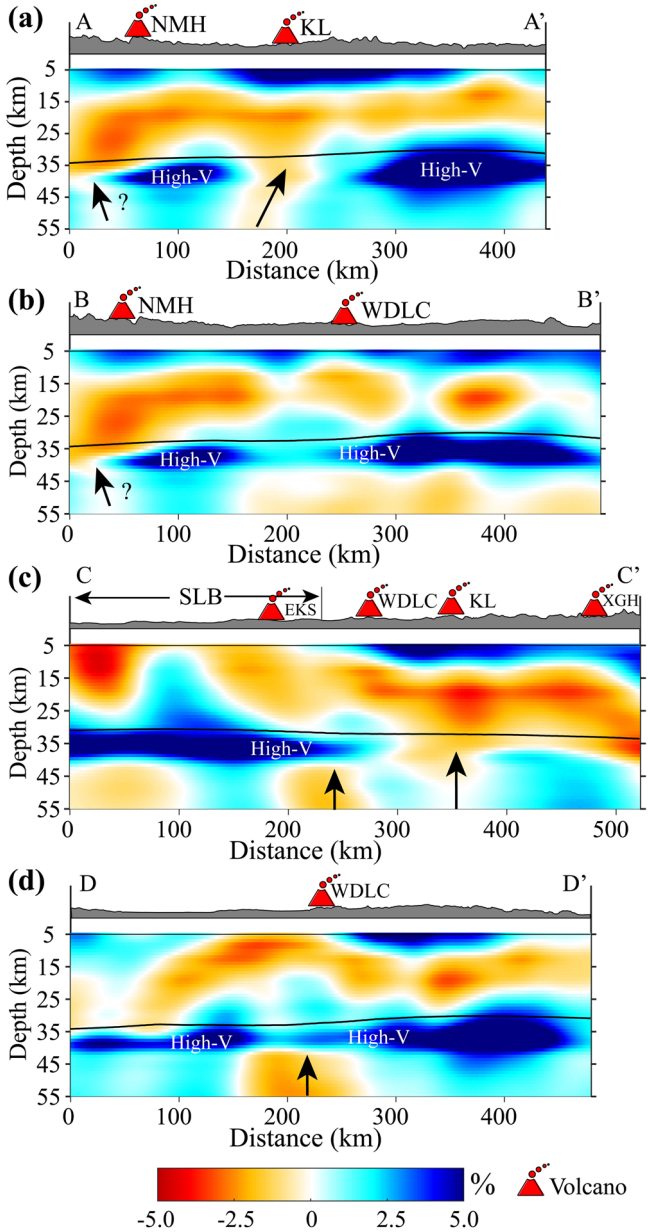

Fig. 3 | Vertical cross-sections of the shear-wave velocity model. a–d Velocity anomalies along different profiles. The black line in each panel denotes the Moho discontinuity[33]. See Fig. 2d for the profile locations. The surface topography is shown atop each cross-section. Other symbols are the same as in Fig. 1. The black arrows depict vertical magmatic pathways based on our tomographic images. High-V denotes a high-velocity anomaly.

crust-mantle boundary (Supplementary Figs. 12–14). The test results show that the recovered anomalies can be clearly distinguished with a minor degree of unavoidable velocity smearing. The observed key structural features under the potassic volcanoes are robust, thanks to the densely deployed seismic stations. Note that the previous regional-scale seismic images with lower resolution could not reveal the vertical magmatic pathways beneath the potassic volcanoes[21,22].

Magmatic plumbing systems of the WDLC volcanic region

Compared to the widespread upper mantle low-V anomalies revealed by large-scale tomographic studies[39,40], our high-resolution Vs tomography resolves a detailed 3-D architecture of trans-crustal magma systems beneath the entire potassic volcanic units. The most conspicuous characteristic in the middle-lower crust is a horizontally ~15-km-thick interconnected low-V zone that is clearly located beneath the XGH-KL-WDLC-EKS volcanic belt (Fig. 3c). Obtaining a more precise geometry of the low-V zone has new implications for understanding the magmatic processes. High crustal temperature and partial melting are the most likely factors to interpret the presence of such a low-V body. The WDLC volcano is characterized by low surface heat flow (~44 mW/m^2)[41], suggesting that the volcano does not release an amount of heat. However, the estimated melt fraction of the magma reservoir in the middle crust is >~15%, with an approximate water content of ~2.1%[20]. Therefore, we suggest that the low-V zone probably reflects magmatic plumbing systems that are connected horizontally with melts and/or fluids moving directly among the potassic volcanic units. Thus, our Vs tomography provides direct seismic evidence for a horizontally extensive magmatic plumbing system in the crust, which may play an important role in the magmatic migration and chemical evolution between the potassic volcanic units.

Rocks from the WDLC volcanic region are all characterized by high potassium contents and enriched Sr-Nd isotopic compositions, suggesting that they may have been derived from a common mantle source[42–44]. The seismic evidence presented in this study for the interconnected magmatic system beneath individual volcanoes is consistent with the previous petrogenetic assessment. The magma source has been proposed either within the lithospheric mantle[45], or from the mantle transition zone associated with the stagnation of the deeply subducted western Pacific slab[10,11,43,46]. However, the stagnant slab is widespread in the mantle transition zone under East Asia, to the east of the North-South Gravity Lineament[14], and the volcanism in this broad region contains both sodic and potassic rocks. It is unclear how the deeply seated slab could control the composition of the erupted volcanics, and high-resolution mantle tomography obtained by a joint inversion of surface-wave and body-wave data may help resolve this issue. Other studies attributed the compositional variation in these highly potassic basalts to the lithospheric thickness variation and lithosphere-asthenosphere interaction[47–50]. Nevertheless, it is challenging to reconcile the origin of the concentrated potassic volcanic clusters with the extensive structural variations observed in the lithospheric mantle and mantle transition zone in northeast China[15,51].

Previous seismic tomographic studies could not elucidate well the relationship between the crustal heterogeneity and spatial distribution of potassic basalts due to the sparse distribution of seismic stations[21,22,39,40]. The densely deployed WAVESArray stations in the WDLC volcanic region led to an obvious improvement in deep seismic imaging. In particular, we are able to detect the interconnected low-V zone in the middle-lower crust. Based on this new finding and the common mantle source hypothesis, we propose a new scenario for the genesis of the potassic intraplate volcanism in northeast China. The crustal interconnected low-V zone may represent remnant magma pathways that transport the metasomatized potassium-rich melts, which appears to promote chemical homogeneity as time progresses among the potassic volcanic units. Although the NMH, KL, WDLC, and EKS volcanic rocks are all classified as potassic series ($1 < K_2O/Na_2O < 2$) in composition[2], the NMH volcano exhibits an obviously lower K_2O/Na_2O ratios[52,53] (Fig. 1b). A longer duration of melt-rock interaction would lead to lower K_2O/Na_2O, $^{87}Sr/^{86}Sr$ ratio, and Rb/Nb ratios[54] (Supplementary Fig. 15). The variations in composition suggest that the NMH volcano underwent longer duration of melt-rock interaction during potassic melt ascent, resulting in increased K consumption and subsequently lower K_2O/Na_2O in the residual melts[54]. Coincidently, the structural features resolved by our Vs tomography beneath these potassic volcanoes are obviously different. For instance, we observe a direct vertical magmatic pathway ascending from the uppermost mantle beneath the KL volcano and a weaker vertical magmatic pathway beneath the NMH volcano (Fig. 3a). The weaker vertical magmatic pathway beneath the NMH volcano could increase the periods of melt-rock interaction, corresponding to a reduction of the K_2O/Na_2O ratio. By contrast, there is no low-V anomaly extending toward the underlying crust right below the WDLC volcano, whereas strong high-V anomalies are mainly located in the uppermost mantle and extend from the SLB to the WDLC volcano (Fig. 3d), which seem to act as barriers preventing magma ascending

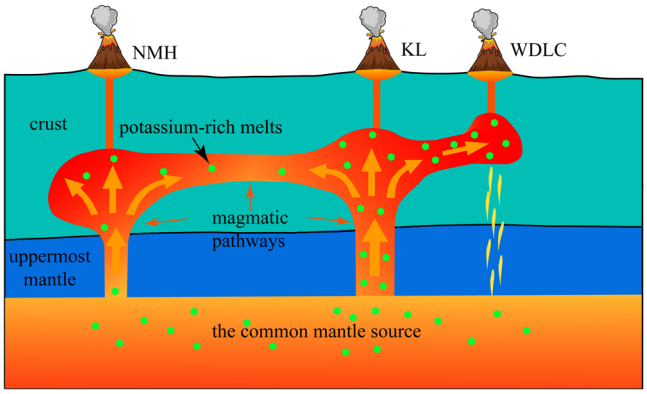

Fig. 4 | A schematic diagram of trans-crustal magmatic systems beneath the potassic intraplate volcanoes in northeast China. The geometries of the magma storage and plumbing systems are simplified. Two vertical magmatic pathways ascend from a common mantle source extending to the middle crust beneath the NMH and KL volcanoes, and the horizontal crustal magmatic pathways transport the potassium-rich melts directly among the potassic volcanic groups.

directly below the WDLC volcano. In the new scenario, based on the correlation between seismic structure and geochemical composition, we suggest that the more active vertical crust-mantle magmatic pathways could decrease the period of melt-rock interaction, corresponding to an increase in K_2O/Na_2O ratio. Moreover, the horizontal interconnected low-V zone in the crust can facilitate direct transfer of potassium-rich magma between the three neighboring volcanoes (KL, WDLC, and EKS), which can well explain the existence of the localized volcanoes with similar potassium contents during the magma compositional evolution.

Trans-crustal magmatic systems of the WDLC potassic volcanic region

The conceptual models of volcanism have evolved from the initial melt-dominated magma chamber to the trans-crustal magmatic systems. The new trans-crustal magmatic systems describe the vertically extensive magma storage[17], including mantle-derived melts, middle-lower crustal reservoirs, and upper crustal pre-eruptive chambers. However, such a hypothesized model is rarely testified in nature probably because of the complexity of magmatic systems and insufficient resolution of seismic detection. The potassic volcanic units host unique vertical and horizontal magma plumbing systems (Fig. 4), providing invaluable seismic evidence for verifying the trans-crustal magmatic conceptual model in northeast China. Two vertical low-V anomalies occur in the uppermost mantle beneath the NMH and KL volcanoes, representing the magma ascending pathways connecting the mantle source and crustal reservoirs. By contrast, in the middle-lower crust, the most conspicuous seismic characteristic is the horizontal interconnected low-V zone at depths of ~15–30 km among the potassic volcanic units, which provides pathways for migrating magmatic melts and facilitates the exchange of chemical composition among the potassic volcanoes. Interestingly, the middle-upper crustal magma reservoirs of the latest erupted WDLC volcano appear to be recharged by the deeper and larger KL crustal magma reservoirs through the horizontally interconnected magmatic pathways. Here, the newly observed magmatic structures provide additional information on the trans-crustal magmatic system model as proposed by Cashman et al.[17]. This magmatic system model emphasizes the vertical multiphase magmatic systems where the magma migrates upwards, and the deeper magma reservoirs recharge the shallow magma reservoirs incrementally. Our high-resolution tomography suggests that the horizontal magmatic plumbing systems may be another way to deliver the magma between the WDLC and KL volcanoes. The horizontal plumbing may be created by crustal extension in northeast China during the late Mesozoic, which is also supported by previous multimodal Rayleigh-wave tomography[55] illustrating a widespread mid-crustal low-V layer in northest China. This resulted in the deformation of a weak middle-lower crust, forming the crystallographic preferred orientation of the middle-lower crustal minerals. This geological process could be influenced by the northwestward subduction of the Paleo-Pacific plate and the closure of the Mongol-Okhotsk Sea in the north[1,3]. The lateral movement of melts could be further powered by the dynamic force associated with the hot upwelling. When the upward-moving melts are reactive and rapidly ascend to the shallow crust of the latest erupted WDLC volcano, the deeper and larger KL magma reservoirs may recharge the WDLC middle-crust magma reservoirs to achieve mass balance through the horizontal interconnected magmatic pathways. Thus, the horizontal magmatic plumbing systems are not only conducive to the magmatic movements, but also can well explain the similar geochemical signatures observed among the potassic volcanic units. Furthermore, from the volcanic hazard perspective, although the WDLC is currently the most active volcano in this region, it is important to pay close attention to the larger crustal magma reservoirs beneath the KL volcano due to their potential hazard. Integrated multidisciplinary investigations and 3-D numerical modeling are highly desirable in the future, in particular, in the monitoring and mitigation of volcanic hazards.

In summary, our high-resolution tomography reveals a robust 3-D architecture of the trans-crustal magmatic systems beneath the potassic volcanic units in northeast China. The vertical magmatic pathways linking the uppermost mantle and crust promote the interaction between the mantle source and the crustal reservoirs beneath the NMH and KL volcanoes. The interconnected low-V zone in the middle-lower crust could transport melts horizontally, responsible for the formation of chemical homogeneity among the potassic volcanic units. These new findings not only provide seismic evidence for the previously hypothesized trans-crustal magmatic concept, but also help better understand the magma storage and migration, as well as the geochemical evolution of the enigmatic intraplate volcanism in northeast China.

Methods

Model parameterization and finite-difference wave simulation

The initial 3-D reference model is derived from a 3-D Vs model parameterized with a lateral grid interval of 0.5° beneath mainland China[32]. The initial model grid extends from 45° to 53° north latitude (~668 km), and from 120° to 132° east longitude (~878 km), and from the Earth's surface down to 199 km depth with a vertical grid interval of 0.5 km. To improve the efficiency of the finite-difference algorithm, we use a non-uniform grid interval to discretize the computational domain. The lateral grid interval is 0.025° in both the longitudinal and latitudinal directions, and the vertical grid size varies continuously with a smaller interval in shallow layers and increases with depth. The Vp and density in the initial model are derived from empirical relationships[56]. We use a non-staggered-grid finite-difference method to simulate waveform propagation in the 3-D heterogeneous Earth's structure[57]. The synthetic waveforms are calculated using a Gaussian pulse acting as the source-time function at each station. The updated synthetic waveforms are calculated for the iteratively updated 3-D velocity model during each iteration. In terms of the longest inter-station distance in the study, we run a total of 2000 steps with a time step of 0.15 s to simulate 300 s wave propagation time.

3-D finite-frequency sensitivity kernels and joint inversion

The 3-D finite-frequency sensitivities of the Rayleigh wave are calculated at each period band using the scattering-integral method[31], which can be used to resolve an accurate high-resolution 3-D velocity model in comparison with the ray theory. We consider the sensitivity kernels for both Vp and Vs in the joint inversion, which can provide more constraints on the shallow crustal structure and obtain more accurate and robust solutions for the deep structures. The phase delay time δt is determined by a joint Vp and Vs inversion,

$$\delta t = \int [K_\alpha(\mathrm{m}_0, x)\Delta \mathrm{m}_\alpha + K_\beta(\mathrm{m}_0, x)\Delta \mathrm{m}_\beta] dV \quad (1)$$

where m_0 is the 3-D reference velocity model, K_α and K_β are 3-D Rayleigh wave sensitivity kernels to Vp and Vs, respectively, and Δm_α and Δm_β are Vp and Vs perturbations at each grid node. The joint inversion is conducted using the LSQR algorithm with a series of damping and smoothing constraints[58].

Data availability

The seismic waveform data used in the study and the obtained 3-D Vs model are archived on the webpage (https://doi.org/10.5281/zenodo.7780684)[59].

Code availability

The codes available for full-wave ambient noise tomography are archived in a repository (https://doi.org/10.5281/zenodo.13117863)[60].

Received: 4 June 2024; Accepted: 30 September 2024;
Published online: 09 October 2024

References

1. Liu, J., Han, J. & Fyfe, W. Cenozoic episodic volcanism and continental rifting in Northeast China and possible link to Japan Sea development as revealed from K-Ar geochronology. *Tectonophysics* **339**, 385–401 (2001).
2. Foley, S. F., Venturelli, G., Green, D. H. & Toscani, L. The ultrapotassic rocks: characteristics, classification, and constraints for petrogenetic models. *Earth-Sci. Rev.* **24**, 81–134 (1987).
3. Chu, Z. et al. Source of highly potassic basalts in Northeast China: evidence from Re-Os, Sr-Nd-Hf isotopes and PGE geochemistry. *Chem. Geol.* **357**, 52–66 (2013).
4. Liu, J. et al. The role of melt-rock interaction in the formation of Quaternary high-MgO potassic basalt from the Greater Khingan Range, northeast China. *J. Geophys. Res. Solid Earth* **122**, 262–280 (2017).
5. Xu, Z. et al. U-Pb geochronology and geochemistry of dikes in the Changbaishan Tianchi volcanic field (NE China) and their relations with the coeval Jingbohu and Longgang monogenetic volcanic fields. *Int. Geol. Rev.* **66**, 814–831 (2023).
6. Xu, Z. et al. Apatite geochemical and Nd isotopic insights into trachyte petrogenesis in the Tianchi volcanic area of Changbai mountain, NE China. *Acta. Geol. Sin-Engl.* **97**, 1671–1682 (2023).
7. Gao, W., Li, J., Mao, X. & Li, H. Geological and geomorphological value of the monogenetic volcanoes in Wudalianchi National Park, NE China. *Geoheritage* **5**, 73–85 (2013).
8. Rasskazov, S. V. et al. Sources of Quaternary potassic volcanic rocks from Wudalianchi, China: control by transtension at the lithosphere-asthenosphere boundary layer. *Geodyn. Tectonophys.* **7**, 555–592 (2016).
9. Zhao, Y., Li, N., Fan, Q., Zou, H. & Xu, Y. Two episodes of volcanism in the Wudalianchi volcanic belt, NE China: evidence for tectonic controls on volcanic activities. *J. Volcanol. Geoth. Res.* **285**, 170–179 (2014).
10. Lei, J. & Zhao, D. P-wave tomography and origin of the Changbai intraplate volcano in Northeast Asia. *Tectonophysics* **397**, 281–295 (2005).
11. Zhao, D., Tian, Y., Lei, J., Liu, L. & Zheng, S. Seismic image and origin of the Changbai intraplate volcano in East Asia: role of big mantle wedge above the stagnant Pacific slab. *Phys. Earth Planet. Inter.* **173**, 197–206 (2009).
12. Guo, Z. et al. Seismic evidence of ongoing sublithosphere upper mantle convection for intraplate volcanism in Northeast China. *Earth Planet. Sci. Lett.* **433**, 31–43 (2016).
13. Lu, M. et al. SKS splitting measurements in NE China: new insights into the Wudalianchi intraplate volcanism and mantle dynamics. *J. Geophys. Res. Solid Earth* **125**, e2019JB018575 (2020).
14. Huang, J. & Zhao, D. High-resolution mantle tomography of China and surrounding regions. *J. Geophys. Res.* **111**, B09305 (2006).
15. Zhao, D. Seismic imaging of Northwest Pacific and East Asia: new insight into volcanism, seismogenesis and geodynamics. *Earth-Sci. Rev.* **214**, 103507 (2021).
16. Du, M., Lei, J., Zhao, D. & Lu, H. Pn anisotropic tomography of Northeast Asia: new insight into subduction dynamics and volcanism. *J. Geophys. Res. Solid Earth* **127**, e2021JB023080 (2022).
17. Cashman, K. V., Sparks, R. S. J. & Blundy, J. D. Vertically extensive and unstable magmatic systems: a unified view of igneous processes. *Science* **355**, eaag3055 (2017).
18. Li, Z. et al. Shallow magma chamber under the Wudalianchi Volcanic Field unveiled by seismic imaging with dense array. *Geophys. Res. Lett.* **43**, 4954–4961 (2016).
19. Zhan, Y. et al. Crustal electric conductivity structure for Wudalianchi volcanic cluster in the Heilongjiang Province. *China. Acta. Petrol. Sin.* **22**, 1494–1502 (2006).
20. Gao, J. et al. Magma recharging beneath the Weishan volcano of the intraplate Wudalianchi volcanic field, Northeast China, implied from 3-D magnetotelluric imaging. *Geology* **48**, 913–918 (2020).
21. Fan, X. et al. Quaternary sodic and potassic intraplate volcanism in Northeast China controlled by the underlying heterogeneous lithospheric structures. *Geology* **49**, 1260–1264 (2021).
22. Chen, Y., Ai, Y., Jiang, M., Yang, Y. & Lei, J. New insights into potassic intraplate volcanism in Northeast China from joint tomography of ambient noise and teleseismic surface waves. *J. Geophys. Res. Solid Earth* **126**, e2021JB021856 (2021).
23. Nolet, G. & Dahlen, F. Wave front healing and the evolution of seismic delay times. *J. Geophys. Res.* **105**, 19043–19054 (2000).
24. Maguire, R. et al. Resolving continental magma reservoirs with 3D surface wave tomography. *Geochem. Geophys. Geosyst.* **23**, e2022GC010446 (2022).
25. Gao, H. & Shen, Y. Upper mantle structure of the Cascades from full-wave ambient noise tomography: Evidence for 3D mantle upwelling in the back-arc. *Earth Planet. Sci. Lett.* **390**, 222–233 (2014).
26. Gao, H. Three-dimensional variations of the slab geometry correlate with earthquake distributions at the Cascadia subduction system. *Nat. Commun.* **9**, 1204 (2018).
27. Lü, Z. et al. Crustal and upper mantle structure of the Tien Shan orogenic belt from full-wave ambient noise tomography. *J. Geophys. Res. Solid Earth* **124**, 3987–4000 (2019).
28. Lü, Z. & Lei, J. Seismic evidence for crustal modification across the Tanlu fault zone in eastern China. *Geophys. Res. Lett.* **49**, e2022GL099761 (2022).
29. Lü, Z. et al. Crustal deformation of intermontane basins beneath Central Tien Shan revealed by full-wave ambient noise tomography. *Tectonophysics* **821**, 229143 (2021).
30. Shen, Y., Ren, Y., Gao, H. & Savage, B. An improved method to extract very-broadband empirical Green's functions from ambient seismic noise. *Bull. Seism. Soc. Am.* **102**, 1872–1877 (2012).
31. Zhao, L., Jordan, T. H., Olsen, K. B. & Chen, P. Fréchet kernels for imaging regional earth structure based on three-dimensional reference models. *Bull. Seism. Soc. Am.* **95**, 2066–2080 (2005).
32. Shen, W. et al. A seismic reference model for the crust and uppermost mantle beneath China from surface wave dispersion. *Geophys. J. Int.* **206**, 954–979 (2016).
33. Zhang, B. et al. Detailed Moho variations under Northeast China inferred from receiver function analyses and their tectonic implications. *Phys. Earth Planet. Int.* **300**, 106448 (2020).
34. Tao, K. et al. Crustal structure beneath NE China imaged by NECESSArray receiver function data. *Earth Planet. Sci. Lett.* **398**, 48–57 (2014).
35. Xie, Z., Wu, Q., Zhou, S. & Zhu, M. Study of crustal thickness and Vp/Vs ratio beneath the Nuomin River volcanoes. *Chinese J. Geophys-ch.* **61**, 4805–4816 (2018).

36. Wei, H., Liu, J. L. & Meng, Q. Structural and sedimentary evolution of the southern Songliao Basin, northeast China, and implications for hydrocarbon prospectivity. *Am. Assoc. Pet. Geol. Bull.* **94**, 533–566 (2010).
37. Liu, Y., Niu, F., Chen, M. & Yang, W. 3-D crustal and uppermost mantle structure beneath NE China revealed by ambient noise adjoint tomography. *Earth Planet. Sci. Lett.* **461**, 20–29 (2017).
38. Yang, Y. et al. Crustal structure beneath Northeast China from ambient noise tomography. *Phys. Earth Planet. Int.* **293**, 106257 (2019).
39. Wei, W. et al. Seismic evidence for a mantle transition zone origin of the Wudalianchi and Halaha volcanoes in Northeast China. *Geochem. Geophys. Geosyst.* **20**, 398–416 (2019).
40. Zhang, F., Wu, Q., Li, Y. & Zhang, R. The seismic evidence of velocity variation for Changbaishan volcanism in Northeast China. *Geophys. J. Int.* **218**, 283–294 (2019).
41. Sun, Y., Dong, S., Zhang, H., Li, H. & Shi, Y. 3D thermal structure of the continental lithosphere beneath China and adjacent regions. *J. Asian Earth Sci.* **62**, 697–704 (2013).
42. Zhang, L., Prelevic, D., Li, N., Mertz-Kraus, R. & Buhre, S. Variation of olivine composition in the volcanic rocks in the Songliao basin, NE China: lithosphere control on the origin of the K-rich intraplate mafic lavas. *Lithos* **262**, 153–168 (2016).
43. Wang, X. et al. Mantle transition zone–derived EM1 component beneath NE China: geochemical evidence from Cenozoic potassic basalts. *Earth Planet. Sci. Lett.* **465**, 16–28 (2017).
44. Ma, L. et al. Molybdenum isotopic constraints on the origin of EM1-type continental intraplate basalts. *Geochim. Cosmochim. Ac.* **317**, 255–268 (2022).
45. Zhang, M., Menzies, M., Suddaby, P. & Thirlwall, M. EM1 signature from within the post-Archaean subcontinental lithospheric mantle: Isotopic evidence from the potassic volcanic rocks in NE China. *Geochem. J.* **25**, 387–398 (1991).
46. Kuritani, T., Kimura, J., Ohtani, E., Miyamoto, H. & Furuyama, K. Transition zone origin of potassic basalts from Wudalianchi volcano, Northeast China. *Lithos* **156**, 1–12 (2013).
47. Guo, P., Niu, Y., Sun, P., Gong, H. & Wang, X. Lithosphere thickness controls continental basalt compositions: an illustration using Cenozoic basalts from eastern China. *Geology* **48**, 128–133 (2020).
48. Niu, Y. Lithosphere thickness controls the extent of mantle melting, depth of melt extraction and basalt compositions in all tectonic settings on Earth—A review and new perspectives. *Earth-Sci. Rev.* **217**, 103614 (2021).
49. Zhang, A. et al. Lithosphere–asthenosphere interactions beneath Northeast China and the origin of its intraplate volcanism. *Geology* **50**, 210–215 (2021).
50. Tian, H., Yang, W., Li, S., Ke, S. & Chu, Z. Origin of low δ^{26}Mg basalts with EM-I component: evidence for interaction between enriched lithosphere and carbonated asthenosphere. *Geochim. Cosmochim. Ac.* **188**, 93–105 (2016).
51. Yang, J. & Faccenda, M. Intraplate volcanism originating from upwelling hydrous mantle transition zone. *Nature* **579**, 88–91 (2020).
52. Sun, Y. et al. Geochemistry of ultrapotassic volcanic rocks in Xiaogulihe NE China: implications for the role of ancient subducted sediments. *Lithos* **208-209**, 53–66 (2014).
53. Sun, Y. et al. Magnesium isotopic evidence for ancient subducted oceanic crust in LOMU-Like potassium-rich volcanic rocks. *J. Geophys. Res. Solid Earth* **122**, 7562–7572 (2017).
54. Liu, J. et al. Lithospheric thickness controlled compositional variations in potassic basalts of Northeast China by melt-rock interactions. *Geophys. Res. Lett.* **43**, 2582–2589 (2016).
55. Zhan, W., Pan, L. & Chen, X. A widespread mid-crustal low-velocity layer beneath Northeast China revealed by the multimodal inversion of Rayleigh waves from ambient seismic noise. *J. Asian Earth Sci.* **196**, 104372 (2020).
56. Brocher, T. Empirical relations between elastic wavespeeds and density in the Earth's crust. *Bull. Seism. Soc. Am.* **95**, 2081–2092 (2005).
57. Zhang, W., Shen, Y. & Zhao, L. Three-dimensional anisotropic seismic wave modeling in spherical coordinate by a collocated-grid finite difference method. *Geophys. J. Int.* **188**, 1359–1381 (2012).
58. Paige, C. & Saunders, M. LSQR: An algorithm for sparse linear equations and sparse least squares. *ACM. Trans. Math. Software.* **8**, 43–71 (1982).
59. Lü, Z. et al. Data for "The magmatic plumbing beneath the Wudalianchi volcanic region, northeast China, is recharged by magma reservoirs under Keluo volcano" [Data set]. Zenodo. https://doi.org/10.5281/zenodo.7780684 (2024).
60. Lü, Z. et al. Codes for "The magmatic plumbing beneath the Wudalianchi volcanic region, northeast China, is recharged by magma reservoirs under Keluo volcano". Zenodo. https://doi.org/10.5281/zenodo.13117863 (2024).

Acknowledgements

We thank all the members who participated in the fieldwork in northeast China. We are very grateful to Dr. Haiying Gao for her help in finite-difference wave simulation. This research was supported by the National Natural Science Foundation of China (U1939206, 42274129, 41530212, 41474040, and 41674091), the Innovation Team Project from National Institute of Natural Hazards, Ministry of Emergency Management of China (2023-JBKY-55), and Research grants from National Institute of Natural Hazards, Ministry of Emergency Management of China (Grant Number: ZDJ2024-28). Prof. (Dr.) Tuncay Taymaz thanks Istanbul Technical University, Rectorate Scientific Research Projects Funding Office (ITU-BAP) for supporting this study. We thank Dr. Carolina Ortiz Guerrero (the editor), Dr. Catherine Annen, and three anonymous reviewers for providing constructive comments and suggestions, which improved the manuscript.

Author contributions

Z.L. processed the seismic data and performed the inversion. Z.L., J.L., D.Z., Y.X., L.L, C.S., Y.A., and T.T. analyzed the results. Z.L. and J.L. proposed the preferred interpretation and discussed with D.Z., Y.X., L.L., and T.T. on the alternative explanations. All authors discussed the results and edited the manuscript.

Competing interests

The authors declare no competing interests.

Additional information

Supplementary information The online version contains supplementary material available at https://doi.org/10.1038/s43247-024-01748-2.

Correspondence and requests for materials should be addressed to Jianshe Lei.

Peer review information *Communications Earth & Environment* thanks Catherine Annen and the other, anonymous, reviewer(s) for their contribution to the peer review of this work. Primary Handling Editors: Domenico Doronzo and Carolina Ortiz Guerrero. A peer review file is available.